Photoconductivity in aligned CdSe nanorod arrays

D. Steiner,[1] D. Azulay,[1] A. Aharoni,[2] A. Salant,[2] U. Banin,[2] and O. Millo[1,*]
[1]*Racah Institute of Physics and the Center for Nanoscience and Nanotechnology, The Hebrew University, Jerusalem 91904, Israel*
[2]*Institute of Chemistry and the Center for Nanoscience and Nanotechnology, The Hebrew University, Jerusalem 91904, Israel*
(Received 1 September 2009; revised manuscript received 15 October 2009; published 11 November 2009)

The voltage dependence of the phototransport in colloidal CdSe nanorods (NRs) arrays was studied for different capping molecules and degree of NR alignment. The photocurrent was found to considerably enhance by exchanging the trioctylphosphine capping ligands by diamine molecules or upon annealing. The corresponding current-voltage characteristics were highly nonlinear, showing, in the aligned NR arrays, a notable decrease in the differential conductivity at a certain capping-molecule-dependent applied electrical field. This transition smears, however, when the degree of NR alignment is reduced. These findings are well described by an exciton field-ionization model, which also accounts for the correlation we observe between the photocurrent $I(V)$ curves and the voltage dependence of the fluorescence quenching in seeded-grown CdSe/CdS core/shell NR films.

DOI: 10.1103/PhysRevB.80.195308 PACS number(s): 73.63.Bd, 72.40.+w, 73.23.−b

I. INTRODUCTION

The conductivity and photoconductivity through arrays of semiconductor nanocrystals (NCs), either two or three dimensional, are of interest both from the fundamental viewpoint and for various applications in optoelectronics, including light emitting diodes,[1–5] photodetectors,[6–8] and photovoltaic cells.[9–11] The discrete, size-dependent energy-level structure of colloidal NCs together with their ability to self-assemble into densely packed arrays make them promising building blocks for fabrication of such devices, as well as for investigating the electronic and optical properties of the intriguing "NCs-solid" phase.[12] The physical properties of the NC solids are easily controlled by modifying the size, shape, and chemical composition of the NCs, as well as the surface ligands, which determine the distance and bridge characteristics, and consequently the electrical coupling between adjacent NCs. Enhancing the inter-NC coupling was found to result in band-gap reduction[13,14] and is obviously expected to significantly enhance the conductivity through the array. Studies of transport and phototransport in arrays comprising spherical quantum dots (QDs) have already been performed for CdSe,[15–21] PbSe,[22–27] ZnO,[28] and CdTe (Ref. 29) "QD solids." Several studies were reported also for randomly oriented nanorod (NR) assemblies.[9,10,30,31] However, the transport properties of aligned NRs arrays were not investigated yet. Semiconductor NRs have already demonstrated considerable advantages over their QDs counterparts in various aspects, including improved performance in photovoltaic cells on account of better charge transport properties[9,10] and enhanced optical gain as compared to spherical dots while providing polarized lasing.[32] These advantages are expected to be even more pronounced in aligned NRs arrays, making them attractive for future applications.

It has been shown previously that the transport properties of NC films dramatically improve upon treatment with diamine cross-linking molecules,[19,20,22,25] thus facilitating experiments that could advance the understanding of charge transport mechanisms in NCs. In this work we extend the above investigations to arrays of well aligned CdSe NRs having smectic ordering, where the various effects governing the transport are more clearly manifested. By this, further insight into the corresponding transport mechanism is gained, in particular, upon comparison with data acquired on disordered arrays, as shown below. Consistent with previous reports,[19,22,25] the photocurrent was considerably enhanced by exchanging the capping ligands by diamine linker molecules (in particular, hydrazine) or after thermal annealing. The photocurrent-voltage $[I(V)]$ characteristics were highly nonlinear, showing, in the aligned NR arrays, a notable decrease in the differential conductivity at a certain capping-molecule-dependent applied electrical field. This specific electric field was higher and at the same time the photocurrent was lower, for samples treated with 1,4-phenylenediamine molecules or annealed, relative to the hydrazine-treated samples. Altering the excitation intensities and wavelengths, on the other hand, does not affect this transition field nor the general shape of the $I(V)$ curves. Importantly, we found that the sharpness of the transition between the higher to the lower differential conductance regimes is significantly reduced as the degree of NR alignment (and smectic ordering) is reduced. All these observations can be well accounted for by a model based on the assumption that phototransport is governed by exciton filed ionization. This model is also consistent with the correlation we find between the photocurrent I-V characteristic and the voltage dependence of the photoluminescence (PL) quenching in CdSe/CdS QD/NR core/shell NCs.

II. EXPERIMENTAL DETAILS

A. Sample preparation

CdSe NRs, about 30 nm long and 4.3 nm in diameter, were grown using the methods of colloidal nanocrystal synthesis, as described elsewhere.[33,34] The synthesis yields high quality NRs, capped with trioctylphosphine (TOP) ligands and with narrow size distribution of less than 10% in diameter and less than 15% in lengths. Seeded-grown CdSe/CdS

NCs consisting of a 3.6 nm diameter CdSe spherical core embedded inside an elongated CdS shell, 5 nm in diameter and 40 nm long, were prepared as described in Ref. 35. The sample was purified by precipitation from the growth solution with methanol and the precipitate containing NRs was redissolved in toluene, forming a solution used for array formation on the substrate, a surface oxidized *p*-doped Si wafer.

Long-range alignment of CdSe NRs on the oxidized silicon substrate was achieved by inserting a piece of the latter vertically into the NRs solution so that the solution-substrate contact line sweeps down along the substrate during the evaporation process. During the slow evaporation process, long-range directional ordering of the NRs was frequently achieved. Similar process was carried out formerly for metal rods[36] but this is a first use of it for colloidal (semiconductor, in our case) rods on patterned substrates for transport measurements. When deposited on clean unpatterned Si substrates, the corresponding NR assemblies consisted of large domains of NRs aligned parallel to one another in smectic type ordering but spatial variations appeared in the direction of orientation from one domain to another. The evaporation rate, which was controlled by changing the vial aperture, was found to be a crucial parameter determining the array quality and was set to the optimal rate of ~15 nm/s. In addition, high NR concentration (above 0.25 optical density) was found essential for achieving ordered arrays. However, surface contamination as well lithographically patterned surface structure highly perturbed the array formation. After patterning the electrodes on the oxidized Si substrate we found that in most cases the NRs tend to align vertically to the electrodes surface and order in ribbons running parallel to the surface, as shown in Fig. 1(a). Unfortunately, we could not obtain arrays with NRs aligned parallel (ribbons running normal) to the electrodes, irrespective of the orientation of the electrodes compared to the solvent surface.

After the deposition, some of the samples were inserted into a glove box for treatment with diamine linker molecules. For hydrazine treatment,[22] the sample was immersed in 1 M hydrazine solution in tetrahydrofuran solvent for 1 h and rinsed by anhydrous acetonitrile. For treatment with 1,4-phenylenediamine we used acetonitrile as a solvent, with 100 mM solution concentration.[20] In this case, the sample was immersed in 1,4-phenylenediamine solution for 30 min and rinsed with anhydrous acetonitrile. Some (TOP-capped NR) samples were annealed at 200 °C for 2 h under nitrogen flow. All samples were inserted promptly into a vacuum chamber, with minimal exposure to ambient atmosphere, for transport measurements.

For our devices we used heavily doped *p*-type Si substrates with 300 nm surface thermal oxide. Au/Ti electrodes, 20 μm wide, with either 1 or 2 μm spacing and 50 nm thick (45 nm gold deposited on top of a 5-nm-thick Ti adhesion layer), were patterned by conventional *e*-beam lithography and lift off.

B. Transport measurements

All the electrical transport measurements were carried out under nitrogen atmosphere inside a pre-evacuated homemade vacuum chamber. In most of the measurements, the samples were illuminated with 473 nm wavelength diode pumped solid-state (DPSS) laser with typical intensity of 380 mW/cm^2. We used a Keithley 236 electrometer as a voltage supply and DL Instruments model 1211 current preamplifier for current detection. The *I-V* characteristics were taken with source-drain voltage steps of 0.4 V and time intervals of 0.5 s. All measurements were carried out at room temperature.

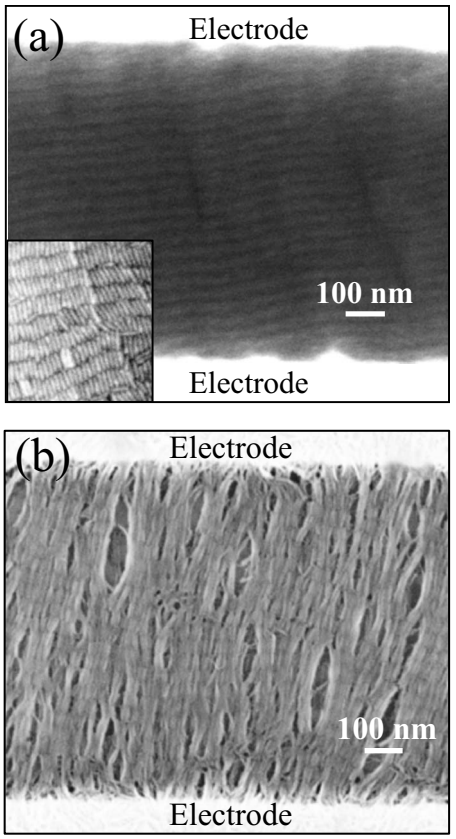

FIG. 1. Scanning electron microscope images of aligned CdSe NRs between gold electrodes (a) before and (b) after treatment with hydrazine. Zoom in to smaller area of aligned NRs is shown in the inset.

C. Photoluminescence intensity measurements

Photoluminescence microscopy was used to study PL quenching of the NRs under applied source-drain voltage. The device structure was the same as that used for the photoconductivity measurements. The NRs were excited by 405 nm wavelength DPSS laser with typical intensity of 1 mW/cm^2. Optical images of the electrodes area were collected by ×100 objective at different source-drain bias voltages (V_{SD}) in the range 0–80 V. The relative fluorescence of the NRs was measured by comparison between the brightness intensity of a defined area between the electrodes before and after applying bias voltage. The voltage was changed in increments of 10 V and was set back to zero after each measurement in order to eliminate the photodegradation contribution to the PL quenching.

III. RESULTS AND DISCUSSION

Figure 1 presents scanning electron microscope (SEM) images of aligned CdSe NRs between gold electrodes (a) before and (b) after treatment with hydrazine. In both cases the NRs are aligned side by side in long ribbons running nearly parallel to the electrodes' edges and the direction of the aligned rods is approximately vertical to them. The side-by-side orientation of the NRs is better demonstrated in the high-resolution SEM image shown in the inset of Fig. 1(a). Although it is difficult to determine the thickness of the NRs film from the SEM images, we estimate that the film contains between two to four layers of aligned NRs. Voids and cracks are seen in the NRs film after treatment with hydrazine [Fig. 1(b)], probably due to the reduction in inter-NR distance during the hydrazine treatment. Voids were observed previously also in hydrazine-treated QD arrays.[22,25] We note in passing, however, that the elongated shape of the voids in our case, compared to these previous works, reflects the present geometry of directional alignment of elongated NRs.

Figure 2(a) shows typical dark-current and photocurrent *I-V* curves of the TOP-capped CdSe NRs. The dark current is very low, only few pA, with linear shape and distinct hysteresis loop, probably due to charging of the nanocrystals. Low dark conductivity implies that the injection of charge carriers from the electrodes to the NRs solid is hindered. This observation is consistent with previous data measured on QD-array systems.[15,18,19] Indeed, it was shown previously that it is difficult to inject electrons into the conduction band and nearly impossible to inject holes into the valence band of CdSe NCs from a gold electrode.[15] The contacts in this situation are referred to as blocking and the only contribution to the photocurrent is therefore from photoexcited charge carriers. The photoconductivity of the TOP-capped NRs was found to be slightly higher than the dark current (about three times larger at the higher voltages) and the nonlinear shape of the *I-V* characteristics suggests some type of interparticle tunneling governed conductance. The relatively low photocurrent of the TOP-capped NRs is attributed to the large spacing between adjacent NRs, (~1.2 nm with TOP molecules) accompanied by high potential barriers for interparticle charge tunneling.

Representative dark-current (blue curve) and photocurrent *I-V* characteristics obtained on hydrazine-treated CdSe NRs array between 1 μm spaced electrodes are presented in Fig. 2(b). While the dark current is still very low, the photoconductivity of the hydrazine-treated NRs is significantly enhanced relative to that of the TOP-capped NRs. This enhancement may be attributed to the reduction in the spacing between the NCs and to the effect of hydrazine induced *n*-type doping, as discussed previously in Refs. 22 and 25, where dramatic enhancement of the conductivity was reported for spherical QDs upon hydrazine treatment. These considerations, however, cannot directly account for the surprising nonlinear shape of the photocurrent *I-V* curve observed for the hydrazine-treated sample. Clear change in the curve slope appears at about $V_{SD}=10$ V, where the voltage dependence of the photocurrent reduces. This is demonstrated even more clearly by the dI/dV vs V curve presented in Fig. 2(c), showing a sharp reduction in the differential

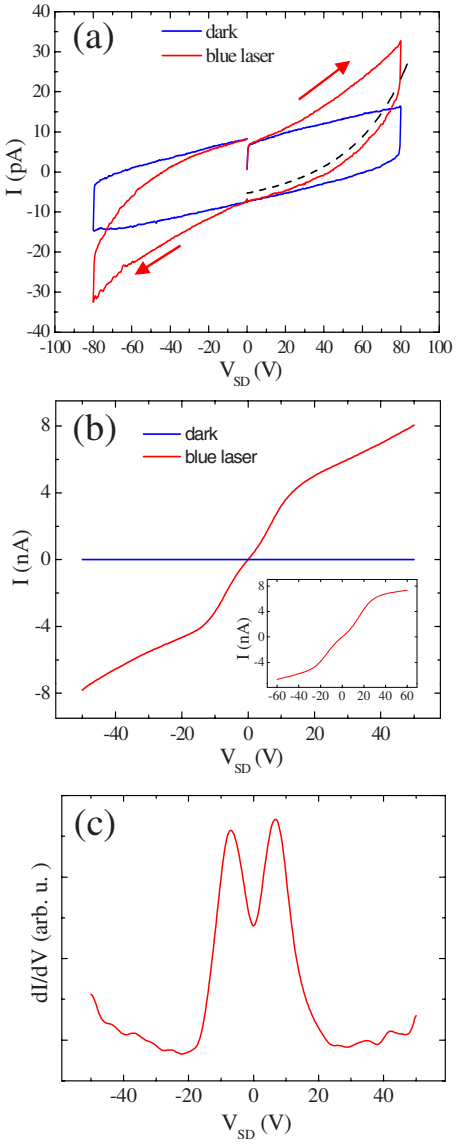

FIG. 2. (Color online) (a) Dark-current (blue curve) and photocurrent *I-V* curves measured on TOP-capped CdSe NRs aligned between 1 μm spaced electrodes. The arrows show the direction of voltage sweep. (b) The same for hydrazine-treated NRs. The inset shows a photocurrent $I(V)$ curve measure with 2 μm spaced electrodes. Note the difference in scale between the different plots. (c) The dI/dV-V characteristics corresponding to the photocurrent curve in (b).

conductivity at around 10 V. This unique photocurrent shape was observed in all measured hydrazine-treated CdSe NRs samples of similar dimensions and, moreover, the typical bias voltage at which the slope changed was found to be approximately the same in all samples of aligned hydrazine-treated CdSe NRs arrays placed between 1 μm spaced electrodes. Importantly, however, this cross-over voltage scaled linearly with the spacing between the electrodes, as demonstrated by the inset of Fig. 2(b) where an $I(V)$ curve taken on a similar array between 2 μm spaced electrodes is presented. This indicates that the change in the *I-V* slope occurs at a specific cross-over electric field E_c or voltage drop per

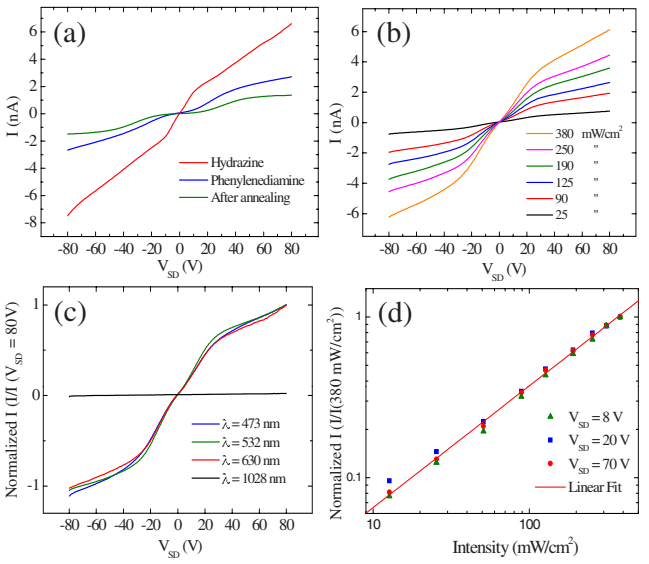

FIG. 3. (Color online) (a) Photo-$I(V)$ characteristics of aligned CdSe NRs arrays after different treatments, as indicated in the figure. (b) Photo-$I(V)$ curves of a hydrazine-treated array under different excitation intensities at $\lambda=473$ nm. (c) Photo-$I(V)$ curves for different excitation wavelengths (normalized to the current at maximal V_{SD}). (d) The dependence of the photocurrent (normalized to the current at maximal excitation intensity) on excitation intensity for three different V_{SD}, all showing power-law behavior.

NR, v_c, which in this system are $\sim 0.7\times 10^5$ V/cm and ~ 0.2 V/particle, respectively.

Further insight into the phototransport mechanisms in aligned NR arrays was gained by studying the dependencies of the photo *I-V* characteristics on other NR surface treatments and excitation wavelength and intensity. The effect of surface treatment on the photocurrent and, in particular, on v_c, was studied here by comparing between the *I-V* curves measured on hydrazine-capped CdSe NRs arrays to those acquired for arrays treated with 1,4-phenylenediamine molecules and for thermally annealed TOP-capped arrays. Figure 3(a) depicts a comparison between these three treatments. All curves exhibit similar nonlinear *I-V* shapes but the photocurrent critical voltage v_c values varied considerably. Interestingly, v_c shifted to higher values as the array photoconductance decreased from the hydrazine capped through the 1,4-phenylenediamine-capped NR arrays, ending with the merely annealed sample. This photocurrent intensity ordering is consistent with the different average interparticle coupling resulting from the different surface treatments, with distance being the smallest ($\sim 3-4$ Å) in arrays where the TOP ligands were exchanged by hydrazine linker molecules and largest (~ 1 nm) in the annealed arrays. This systematic increase in v_c with increased NR separation can be understood within a model presented below. We would like to note here that the annealed and the 1,4-phenylenediamine-treated samples were found to be unstable with time and after 2 or 3 V_{SD} sweeps the photocurrent quenched considerably, in contrast to the very robust hydrazine-treated arrays. Because of the higher photoconductivity and stability of the latter, we chose to continue working mainly with the hydrazine-treated arrays.

Figures 3(b) and 3(c) show a comparison between photocurrent *I-V* curves obtained with different excitation intensities and wavelengths, respectively. It is clearly evident that the shape of the *I-V* curves, as well as cross-over voltage v_c, do not depend on the excitation intensity or photon energy (for supra band-gap excitations). The negligible photocurrent obtained with subband-gap excitation [$\lambda=1028$ nm, see Fig. 3(c)] indicates that charge-carrier photogeneration takes place mainly by band-to-band excitation and the contribution of surface states or capping-molecule related states is negligible. One can thus conclude, based on the data presented here, that the shape of the *I-V* characteristics and, in particular, v_c is an *intrinsic* property of the NRs array.

Another fundamental property of interest here is the dependence of the photocurrent on excitation intensity. This is plotted in Fig. 3(d) on a log-log scale for three different V_{SD} values. The photocurrent shows a power-law dependence on intensity, $I\propto G^{\gamma}$, where G is the generation rate and $\gamma=0.75$ (as extracted from the linear fit). Such a value for the "γ exponent" ($0.5<\gamma<1$), suggests, in bulk systems, the contribution of band tails to photoconductivity.[37] In our system, in turn, this should reflect the contribution of inhomogeneous broadening typical of NC systems. The effect of this broadening on the shape of the *I-V* curves is further discussed below.

Our results are well described by the exciton field-ionization model previously presented by Leatherdale *et al.*[16] According to this model, the photocurrent is governed by the tunneling rate of the field-ionized exciton charges between neighboring NCs. Correspondingly, the photocurrent is determined by three main (sample average) factors: the tunnel barrier height, Φ, the distance between adjacent NCs, d, and the energy difference, Δ, between the initial exciton ground state and the final state where the electron and hole reside on adjacent NCs. One would thus expect that the onset of the current through the array will take place (assuming no level broadening) only when the voltage drop per NC or site-to-site potential, v, will exceed Δ, and therefore $\Delta\approx v_c$. This is indeed directly reflected in the dependence of the tunneling rate, Γ, on v, given by[16]

$$\Gamma(v)\propto \frac{\exp\left(\frac{-4\sqrt{2}\hbar^2 d}{3m(ev-\Delta)}\left\{\left(\frac{m\Phi}{\hbar^2}\right)^{3/2}-\left[\frac{m(\Phi+\Delta-ev)}{\hbar^2}\right]^{3/2}\right\}\right)}{1+\exp\left(-\frac{ev-\Delta}{b}\right)}. \quad (1)$$

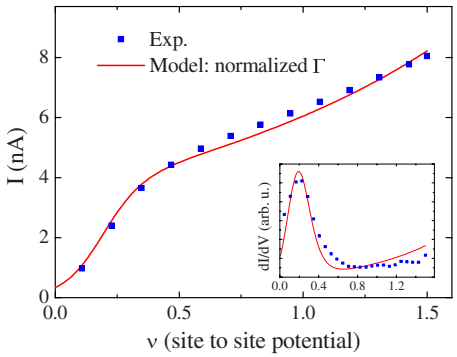

FIG. 4. (Color online) Comparison between the experimental photocurrent shown in Fig. 2(b) and the theoretical curve based on the exciton field-ionization model [Eq. (1)]. The theoretical curve was scaled to fit the photocurrent results. The parameters values used for the calculation are: $\Delta=0.18$ eV, $\Phi=2.3$ eV, $d=3$ Å and $b=0.08$ eV. The inset shows the corresponding dI/dV spectra.

Here, m is the effective mass of the electron and e is the elementary charge. The parameter b describes the amount of effective broadening of Δ due to fluctuations in the NC size and the inter-NC separation, d. This broadening allows photocurrent also for small V_{SD}, where $v<\Delta\sim v_c$. In addition, the broadening washes out any signature of level discreetness in the "global" photo-$I(V)$ curves, which appear to grow smoothly for $v>v_c$, unlike the case of tunneling spectra measured[14] on *single* NCs within an array. Note that the interparticle distance d is expected to affect Δ, thus contributing to $\Gamma(v)$ beyond the trivial exponential dependence of the tunneling rate on distance.

Figure 4 shows an example of a calculated I-v curve based on this model, together with (and normalized to) the experimental photocurrent data already shown in Fig. 2(b). The site-to-site potential, shown in the x axis of Fig. 4, is calculated by assuming that the potential drops uniformly across the spacing between the electrodes and that the rods are oriented exactly parallel to the direction of the applied voltage. A qualitatively good agreement with the experimental data was achieved with $\Phi=2.3$ eV, $d=3$ Å, $\Delta=0.18$ eV, and $b=0.08$ eV, which are reasonable parameters. The short spacing between adjacent NRs, of only 3 Å, is consistent with the previously reported value for hydrazine-treated QDs, based on small-angle x-ray scattering measurements.[25] The values of Φ, Δ, and b are close to those used in the modeling of spherical CdSe QDs,[16] with minor changes probably resulting from differences in shape, orientation, and capping molecules of the NRs studied here.

The exciton field-ionization model enables us to better understand the physical mechanism responsible for the unique shape of the I-V curves measured on aligned NR arrays. As can be seen in Fig. 4, the change in the slope of the curve occurs at a site-to-site potential, that is, very close to Δ (see also the inset of Fig. 4), as anticipated and discussed above. The I-V characteristics [or $\Gamma(v)$] can be separated, therefore, into two well-defined regimes. At low bias voltages, $v<v_c\sim\Delta$, the current grows rapidly with V_{SD} due to the rapid enhancement of the exciton ionization efficiency with voltage; the smaller the broadening parameter b is, the sharper will this process be (and no current is expected for $v<\Delta$ when $b=0$). When $v>\Delta$, the exciton field-ionization process is not energetically hindered any more and the voltage dependence of the photocurrent is governed merely by tunneling between two sites separated by a distance d under the (slightly bias-tilted) potential barrier of height $\sim\Phi$ (where a constant structureless density of states is assumed here above the band edges, as noted above). According to this description, the higher v_c value, together with the lower photocurrent, observed upon treatment with 1,4-phenylenediamine compared to hydrazine-treated arrays [Fig. 3(a)] is due to the relatively large spacing between neighboring NRs in the former samples. Larger d acts not only to reduce the tunneling current, but also to increase Δ, due to the larger electron-hole separation in the final state of exciton ionization. The same considerations obviously hold also for the annealed samples.

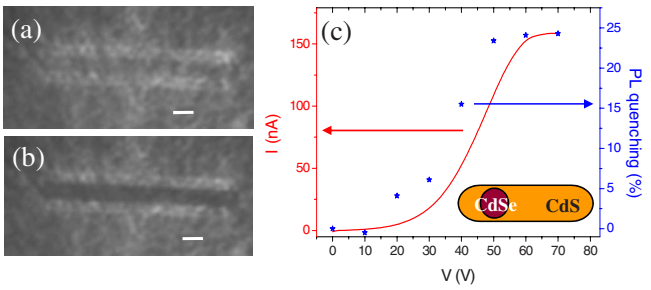

FIG. 5. (Color online) Optical microscope images of the electrodes region over which seeded-grown CdSe/CdS core/shell NRs were deposited and under illumination with (a) no bias voltage and (b) under applied voltage of 60 V. Scale bars are 2 μm. (c) Photoluminescence quenching (blue asterisks) and photocurrent (red line) as a function of applied voltage for the CdSe/CdS NRs assembly.

The exciton field-ionization process described above is expected to quench the PL in such NCs arrays and therefore, to further verify the model, we turned to study the corresponding PL intensity dependence on V_{SD}. The quantum yield of the CdSe NRs is very low and thus we performed this experiment on assemblies of seeded-grown CdSe/CdS QD/NR core/shell NRs. Figures 5(a) and 5(b) show optical microscope pictures of 2 μm spaced electrodes after deposition of CdSe/CdS NRs and under supra band-gap illumination, with zero bias voltage and under applied voltage of 60 V, respectively. The quenching of the fluorescence is clearly seen by darkening of the region between the electrodes [Fig. 5(b)]. Figure 5(c) shows the correlation between the bias-voltage dependence of the PL quenching and the photo-I-V curve measured on TOP-capped CdSe/CdS NRs sample. (The origin for the much larger photocurrent observed here even before any surface treatment, compared to the CdSe NR samples is not yet fully understood, and may be due to the different shell material; note that we observed larger photocurrents also for CdS NRs. This material-related issue will be addressed elsewhere). The similarity between these two dependencies indicates, indeed, that both the photoconductivity and PL quenching in NRs array are controlled by the same physical mechanism, namely, the exciton field ionization while the photocurrent is enhanced as the rate of electron-hole separation increases, the PL is obviously reduced due to such charge separation.

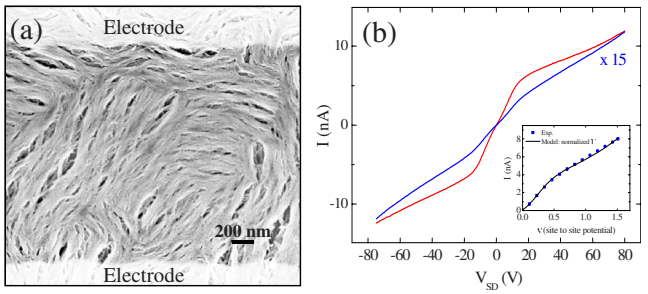

FIG. 6. (Color online) (a) SEM image of randomly aligned hydrazine-treated CdSe NRs between gold electrodes. (b) Comparison between photo-*I*-*V* curves measured on disordered (blue curve) and NRs arrays with smectic order. The blue curve is multiplied by 15 to scale with the red curve. Inset: a comparison between the experimental photocurrent measured on the disordered NR array (plotted as a function of site-to-site potential) and the exciton field-ionization model, Eq. (1) (scaled to fit the photocurrent magnitude). The same fitting parameters as in Fig. 4 were used here, except for the broadening parameter b, which is higher (b=0.14) than that used for the ordered arrays.

The general shape of the *I*-*V* curves observed on the aligned NRs arrays is consistent with previous observations on QD arrays.[16] However, the cross over from the high to low differential conductance regime is much sharper in our case. We assign this to the smectic ordering in the NR arrays: the arrays consist of NR ribbons running nearly parallel to the electrodes, where within each ribbon the NRs are aligned perpendicular to the electrodes. Consequently, the condition that the *local* v exceeds Δ may take place nearly simultaneously (as a function of V_{SD}) for all the NRs, and thus v_c is well defined for a given such array. In some samples, however, the NR deposition did not result in an ordered array and after hydrazine treatment the (much shorter) ribbons arranged in random spaghettilike structures, as shown by Fig. 6(a). (This probably occurred since the corresponding electrode was placed too close the initial solvent surface, so the steady-state conditions needed for ordering were not yet established.[36]) In such an array, the above condition does not hold and the transition is expected to be blurred due to the vast inhomogeneous broadening. Indeed, the *I*-*V* characteristics measured on that (hydrazine-treated) CdSe NR assembly exhibited a smeared transition [blue curve in Fig. 6(b)] compared to that measured on the ordered array (red curve), although the value v_c is comparable between the two. This curve can indeed be well fit to the model using the same parameters as in Fig. 4, except for the broadening parameter which is much larger here, b=0.14. The significantly (order of magnitude) smaller photocurrent observed on the disordered sample results from the strongly meandering ribbon arrangement and the concomitant random directional orientation of the intervening voids, complicating the tunneling-percolation paths between the two electrodes.

IV. CONCLUSIONS

The photoconductivity of aligned CdSe NRs arrays is significantly increased by exchanging the TOP capping ligands by hydrazine or 1,4-phenylenediamine linker molecules or by thermal annealing. The photo-*I*-*V* characteristics of these arrays are nonlinear, and the differential conductance exhibits a transition from higher to lower values as the average voltage drop per NR, or average site-to-site potential, exceeds some array specific value, independent of the excitation wavelength or intensity. The sharpness of this cross over increases with the degree of NR orientation and smectic ordering of the array. All these findings are well described by an exciton field-ionization model proposed previously,[16] the details of which are more clearly demonstrated here via the effects of array ordering and NR surface treatment. The good correlation that was found between the PL quenching as a function of the applied bias and the photo-*I*-*V* curves provides further support to this model.

ACKNOWLEDGMENTS

We thank the staff of the Unit for Nanofabrication of the Center for Nanoscience and Nanotechnology in the Hebrew University, Jerusalem, headed by S. Eliav and, in particular, Yigal Lilach for the EBL work. The research was supported in part by the G.I.F (U.B.) and the Israel Science Foundation—Center of Excellence (O.M.). O.M. acknowledges support from the Harry de Jur Chair in Applied Science. U.B. acknowledges support of the Alfred and Erica Larisch Memorial Chair in Solar Energy.

*Corresponding author; milode@vms.huji.ac.il

[1] V. L. Colvin, M. C. Schlamp, and A. P. Alivisatos, Nature (London) **370**, 354 (1994).
[2] S. Coe, W. K. Woo, M. G. Bawendi, and V. Bulovic, Nature (London) **420**, 800 (2002).
[3] B. O. Dabbousi, M. G. Bawendi, O. Onitsuka, and M. F. Rubner, Appl. Phys. Lett. **66**, 1316 (1995).
[4] M. Gao, C. Lesser, S. Kirstein, H. Möhwald, A. L. Rogach, and H. Weller, J. Appl. Phys. **87**, 2297 (2000).
[5] M. V. Artemyev, V. Sperling, and U. Woggon, J. Appl. Phys. **81**, 6975 (1997).
[6] P. Bhattacharya, A. D. Stiff-Roberts, S. Krishna, and S. Kennerly, Int. J. High Speed Electron. Syst. **12**, 969 (2002).
[7] L. W. Ji, Y. K. Su, S. J. Chang, S. H. Liu, C. K. Wang, S. T. Tsai, T. H. Fang, L. W. Wu, and Q. K. Xue, Solid-State Electron. **47**, 1753 (2003).
[8] G. Konstantatos, I. Howard, A. Fischer, S. Hoogland, J. Clifford, E. Klem, L. Levina, and E. H. Sargent, Nature (London) **442**, 180 (2006).
[9] W. U. Huynh, J. J. Dittmer, and A. P. Alivisatos, Science **295**, 2425 (2002).
[10] W. U. Huynh, J. J. Dittmer, N. Teclemariam, D. J. Milliron, A. P. Alivisatos, and K. W. J. Barnham, Phys. Rev. B **67**, 115326 (2003).

[11] A. J. Nozik, Physica E (Amsterdam) **14**, 115 (2002).
[12] C. B. Murray, C. R. Kagan, and M. G. Bawendi, Annu. Rev. Mater. Sci. **30**, 545 (2000).
[13] P. Liljeroth, P. A. Zeijlmans van Emmichoven, S. G. Hickey, H. Weller, B. Grandidier, G. Allan, and D. Vanmaekelbergh, Phys. Rev. Lett. **95**, 086801 (2005).
[14] D. Steiner, D. Azulai, A. Aharoni, U. Banin, and O. Millo, Nano Lett. **6**, 2201 (2006).
[15] D. S. Ginger and N. C. Greenham, J. Appl. Phys. **87**, 1361 (2000).
[16] C. A. Leatherdale, C. R. Kagan, N. Y. Morgan, S. A. Empedocles, M. A. Kastner, and M. G. Bawendi, Phys. Rev. B **62**, 2669 (2000).
[17] N. Y. Morgan, C. A. Leatherdale, M. Drndić, M. V. Jarosz, M. A. Kastner, and M. Bawendi, Phys. Rev. B **66**, 075339 (2002).
[18] M. Drndić, M. V. Jarosz, N. Y. Morgan, M. A. Kastner, and M. G. Bawendi, J. Appl. Phys. **92**, 7498 (2002).
[19] M. V. Jarosz, V. J. Porter, B. R. Fisher, M. A. Kastner, and M. G. Bawendi, Phys. Rev. B **70**, 195327 (2004).
[20] D. Yu, C. Wang, B. L. Wehrenberg, and P. Guyot-Sionnest, Phys. Rev. Lett. **92**, 216802 (2004).
[21] D. Yu, B. L. Wehrenberg, P. Jha, J. Ma, and P. Guyot-Sionnest, J. Appl. Phys. **99**, 104315 (2006).
[22] D. V. Talapin and C. B. Murray, Science **310**, 86 (2005).
[23] H. E. Romero and M. Drndić, Phys. Rev. Lett. **95**, 156801 (2005).
[24] J. E. Murphy, M. C. Beard, and A. J. Nozik, J. Phys. Chem. B **110**, 25455 (2006).
[25] M. Law, J. M. Luther, Q. Song, B. K. Hughes, C. L. Perkins, and J. Nozik, J. Am. Chem. Soc. **130**, 5974 (2008).
[26] T. S. Mentzel, V. J. Porter, S. Geyer, K. MacLean, M. G. Bawendi, and M. A. Kastner, Phys. Rev. B **77**, 075316 (2008).
[27] R. Y. Wang, J. P. Feser, J. S. Lee, D. V. Talapin, R. Segalman, and A. Majumdar, Nano Lett. **8**, 2283 (2008).
[28] D. Vanmaekelbergh and P. Liljeroth, Chem. Soc. Rev. **34**, 299 (2005).
[29] V. J. Porter, T. Mentzel, S. Charpentier, M. A. Kastner, and M. G. Bawendi, Phys. Rev. B **73**, 155303 (2006).
[30] H. E. Romero, G. Calusine, and M. Drndić, Phys. Rev. B **72**, 235401 (2005).
[31] A. Persano, G. Leo, L. Manna, and A. Cola, J. Appl. Phys. **104**, 074306 (2008).
[32] M. Kazes, D. Y. Lewis, Y. Ebenstein, T. Mokari, and U. Banin, Adv. Mater. (Weinheim, Ger.) **14**, 317 (2002).
[33] X. Peng, L. Manna, W. Yang, J. Wickham, E. Scher, A. Kadavanich, and A. P. Alivisatos, Nature (London) **404**, 59 (2000).
[34] D. Katz, T. Wizansky, O. Millo, E. Rothenberg, T. Mokari, and U. Banin, Phys. Rev. Lett. **89**, 086801 (2002).
[35] L. Carbone, C. Nobile, M. De Giorgi, F. Della Sala, G. Morello, P. Pompa, M. Hytch, E. Snoeck, A. Fiore, I. R. Franchini, M. Nadasan, A. F. Silvestre, L. Chiodo, S. Kudera, R. Cingolani, R. Krahne, and L. Manna, Nano Lett. **7**, 2942 (2007), and supplementary information.
[36] B. Nikoobakht, Z. L. Wang, and M. A. El-Sayed, J. Phys. Chem. B **104**, 8635 (2000).
[37] A. Rose, in *Concepts in Photoconductivity and Allied Problems*, edited by R. E. Marshak (Wiley, New York, 1963).